NIH Public Access
Author Manuscript
J Proteome Res. Author manuscript; available in PMC 2008 December 1.

Published in final edited form as:
J Proteome Res. 2007 December ; 6(12): 4601–4607. doi:10.1021/pr070401e.

Integration of ^{18}O Labeling and Solution Isoelectric Focusing in a Shotgun Analysis of Mitochondrial Proteins

Jinshan Wang[1], **Peter Gutierrez**[2], **Nathan Edwards**[3,*], and **Catherine Fenselau**[1,2,*]

1 *Department of Chemistry and Biochemistry, University of Maryland, College Park, Maryland 20742*

2 *Greenebaum Cancer Center, University of Maryland Medical School, Baltimore, Maryland 21201*

3 *Center for Bioinformatics and Computational Biology, University of Maryland, College Park, Maryland 20742*

Abstract

Forward and reverse ^{18}O labeling are integrated with solution isoelectric focusing and capillary LC-tandem mass spectrometry to evaluate a new strategy for quantitative proteomics, and to study abundance changes in mitochondrial proteins associated with drug resistance in MCF-7 human cancer cells. Galectin-3 binding protein, which is involved in apoptosis, was detected only in the resistant cell line, as a result of reverse labeling. Among 278 proteins identified, twelve were detected with abundances altered at least 2-fold.

Keywords

comparative proteomics; ^{18}O labeling; reverse labeling; solution isoelectric focusing; galectin; 3 binding protein; human mitochondria; drug resistance

INTRODUCTION

The coupling of efficient separations and mass spectrometry instrumentation is highly desirable to provide global proteomic analysis. When quantitative comparisons are part of the strategy, separation and analytical methods should be selected, which optimize the isotope labeling procedure. Enzyme-catalyzed ^{18}O labeling is considered to be advantageous for analysis of proteins from tissue and other limited samples (1–3). However, the introduction of this and other labels at the peptide stage mandates that protein manipulation be minimized in favor of peptide fractionation post-labeling. “Shotgun” strategies (4,5), which rely on the multi-dimensional separation of peptides from digested protein mixtures, are especially suitable for integrating ^{18}O labeling into comparative proteomic analyses.

A variety of approaches, including cation-exchange chromatography (4,5), affinity chromatography (6,7) and electrokinetic-based focusing (8–18), have been proposed as the first dimension separation, followed by reversed-phase liquid chromatography and mass spectrometry analysis. The focusing techniques, including capillary isoelectric focusing (8,9), rotational focusing (10), free-flow electrophoresis (12,13) and multi-compartment electrolyzers (14–18), exploit the same isoelectric focusing principle adopted in the first dimension of a 2-D gel. They are of particular interest since they provide pI-based separation

Contact information: fenselau@umd.edu phone 301-405-8616; fax 301-405-8615, nedwards@umd.edu phone 301-405-9901; fax 301-314-1341.

NIH-PA Author Manuscript
NIH-PA Author Manuscript
NIH-PA Author Manuscript

NIH-PA Author Manuscript

NIH-PA Author Manuscript

NIH-PA Author Manuscript

as another physical characteristic to assist database searching (11), and provide separations in solution, which are more readily automatable.

We have previously established a two-dimensional strategy for nuclear peptide separation (18), which incorporated solution isoelectric focusing (sIEF) with reversed-phase LC-MS/MS. In this method, high loading capacity, high sample recovery and good reproducibility have been shown. In the present study, the sIEF-based strategy has been applied to analyze a soluble mitochondrial fraction isolated from human MCF-7 breast cancer cells. The human mitochondrion is central to basic life functions, including production of cellular energy and apoptosis, and its proteomic heterogeneity in different organs and diseases is currently the focus of intensive study around the world (e.g. 19–26). The organelle naturally emerges as an important target for new proteomic methods.

Alterations in the abundances of proteins in soluble mitochondrial fractions of a drug resistant MCF-7 cell line and its parental drug susceptible cell line were investigated to provide enhanced understanding of drug resistance. ^{18}O labeling was integrated with the 2-D separation strategy described above. Furthermore, both forward and reverse ^{18}O labeling experiments were incorporated to make it possible to check for a systematic bias introduced by labeling in one particular direction. In addition, this strategy facilitates the identification of “on/off” proteins detectable in one cell line, but not the other.

EXPERIMENT SECTION

Materials

Percoll and IPG buffer (pH 3–10) were purchased from Amersham Biosciences (Piscataway, NJ). Micro Bio-Spin 6 chromatography columns were obtained from Bio-Rad (Hercules, CA). PepClean™ C-18 spin columns were purchased from Pierce (Rockford, IL). Multi-compartment electrolyzer (MCE) kit was from Proteome Systems (Woburn, MA). Isotopically enriched $H_2{}^{18}O$ (>95% ^{18}O) came from Isotech, Inc. (Miamisburg, OH). Poroszyme bulk immobilized trypsin was purchased from Applied BioSystems (Foster City, CA). Modified porcine trypsin (sequence grade) was purchased from Promega (Madison, WI). Ultrafiltration membranes (500 Da cut-off) came from Millipore (Billerica, MA). All additional materials were purchased from Sigma-Aldrich (St. Louis, MO).

MCF-7 Cell Culture and Mitochondrial Peptide Preparation

The MCF-7 cell line selected for resistance to mitoxantrone was provided by Dr. Ken Cowan (The Eppley Institute, University of Nebraska Medical Center, Omaha, NE). The drug susceptible MCF-7 cell line used also originated in Dr. Cowan’s laboratory. These were grown on 150 cm^2 flasks in Improved Minimal Essential Media (MEM) solution containing 10% fetal bovine serum and 1% penicillin streptomycin solution at 37°C and 5% CO_2. The cells were harvested at confluence. A mitochondrial isolation kit (Sigma) was used to isolate crude MCF-7 mitochondria according to the manufacturer’s instructions. The mitochondrial pellet was re-suspended in an extraction buffer containing 10mM N-2-hydroxyethylpiperazine-N′-2-ethanesulfonic acid, pH 7.5, 70 mM sucrose, 200mM mannitol and 1mM ethylene glycol-bis (2-aminoethyl ether)-N, N, N′, N′-tetra-acetic acid. One milliliter aliquot of the suspension was loaded in the extraction buffer containing 20ml of 30% Percoll (21). The mixture was spun down at 95000g for 30 minutes. The purified mitochondria were collected from the lower fraction and washed twice by being diluted into a ten-fold volume of extraction buffer and centrifuged at 10000g for 20 minutes. The resulting pellet was re-suspended in 10 mM N-2-hydroxyethylpiperazine-N′-2-ethanesulfonic acid buffer (pH 7.4) and then vortexed vigorously for 15 seconds every 5 minutes, for a total 25 minutes. An equal volume of 1.4 M sucrose was then added to the sample with further incubation for 20 minutes. The resulting mixture was

NIH-PA Author Manuscript

NIH-PA Author Manuscript

NIH-PA Author Manuscript

then subjected to two 15-second bursts of probe sonication with 1-min rests in between. The suspension was centrifuged at 15000g for 15 minutes. The supernatant was diluted with an equal quantity of 100 mM tris[hydroxymethyl]aminomethane buffer (pH 7.5), then centrifuged at 10500g for 50 minutes. The supernatant fraction was collected. The proteins were denatured with 6M urea, reduced with two 45 minute incubations with 10mM dithiothreitol and alkylated by reaction with 100mM iodoacetamide in the dark for 1 hour. The resulting sample was desalted using Bio-Spin 6 size exclusion columns and protein concentration was determined with the Bio-Rad protein assay kit. The sample was then digested by trypsin at 37°C overnight.

Forward and Reverse ^{18}O labeling

Using the previously determined total protein concentration of the proteins harvested from each cell-line, aliquots of approximately 1mg were drawn from wild-type and mitoxantrone resistant peptide preparations, in a 1:1 ratio (by protein mass). To each digested peptide pool, a volume of the clean immobilized trypsin (washed 3X) was added equal to 20% of the sample volume. The mixture was then dried completely. The pool was redissolved in 20% acetonitrile and 80% $H_2{}^{18}O$ (>95% ^{18}O). The unlabeled peptide counterpart was redissolved in 20% acetonitrile and 80% $H_2{}^{16}O$. The solution was rotated at 37°C for approximately 5 hours on a bench-top rotator. The resulting peptide pool was then filtered with a centrifugal filtering device (0.45μm membrane) to remove immobilized trypsin and preclude back exchange. The labeled and unlabeled peptide filtrates were combined and analyzed on the LC-QqTOF instrument. In the forward ^{18}O labeling experiment, peptides from the drug susceptible cell line were labeled with ^{18}O water. In the reversed ^{18}O labeling experiment, peptides from drug resistant cell line were labeled with ^{18}O water.

Biological and Analytical Sample Replicates

Each biological replicate consists of a pair of protein harvests from wild-type (WT) and mitoxantrone resistant (MX) cell lines. The “MCF-7 Cell Culture and Mitochondrial Peptide Preparation” method was carried out independently for each protein harvest. Six aliquot pairs in 1:1 ratio (total protein content, by mass), were drawn from each biological replicate and labeled using the “Forward and Reverse ^{18}O Labeling” method, three in the forward direction, and three in the reverse direction. Two biological replicates were carried out, resulting in 12 analytical samples. Each analytical sample was subjected to solution isoelectric focusing (sIEF) and LC/MS mass spectrometry. Scheme 1 summarizes the analytical sample replicate structure of this experimental design for each biological replicate.

Solution Isoelectric Focusing (sIEF) Separation

Six Teflon dialysis chambers, including four separation chambers and two terminal electrode chambers (500μl volume each), were assembled (Amika Corp., Columbia, MD). Five Immobiline gel membranes having different pH values, 3.0, 5.0, 6.5, 8.0 and 11, from an MCE kit (Proteome Systems, Woburn, MA) were assembled between these chambers. Two ultrafiltration membranes (500Da cut-off) were used for ending the two terminal electrode chambers. The peptide sample was loaded into the chamber with pH 5.0 to 6.5. The two terminal chambers were filled with Electrode Buffer from MCE kit while the other chambers were all filled with Chamber Buffer. The assembled chambers were put into the electrophoresis tank, which was divided into two parts: cathode and anode compartments. Seven mM phosphoric acid was used to fill the anode compartment while 20mM lysine and 20mM arginine solution was used for the cathode compartment. The running program was: 100V for 10 min, 200V for 20 min, 500 V for 40 min and 1000 V for about 100 min. After focusing, fractionated samples from different chambers were collected separately and desalted using PepClean C-18 spin columns (Pierce Chemicals).

NIH-PA Author Manuscript

NIH-PA Author Manuscript

NIH-PA Author Manuscript

MicroLC-Ion trap mass spectrometry

Peptides from an unlabeled sample of drug susceptible MCF-7 cells were fractionated by sIEF and desalted as described above. The sIEF fractions were redissolved in 0.1% formic acid and 10 μl samples of each were placed in the autosampler of the Surveyor HPLC system for automatic injection into an LCQ Decca XP+ ion trap mass spectrometer (ThermoFinnegan, San Jose CA). The reversed-phase separation column was a 75μm ID×10cm fused capillary packed with 300Å BioBasic C18 particles. The peptides were eluted with a gradient of 3–60 % B for 60 min, 60–97% B for 10 min, and 97% B for 10 min at a flow rate of 275 nl/min. Solvent A was water with 0.1% trifluoroacetic acid and solvent B was acetonitrile with 0.1% trifluoroacetic acid. The spray voltage was 2.0 kV. Acquisition of each full mass spectrum was followed by acquisition of MS/MS spectra of the three most intense peaks. Resulting DTA files were merged and searched against the SwissProt human database using a MASCOT in-house search engine. Criteria used for the searches allowed for carbamidomethylation of cysteine as a fixed modification and oxidation of methionine as a variable modification, one missed cleavage of trypsin, and fragment mass tolerance at ±0.8Da. Peptides matched with more than 95% confidence are listed as identified. These significant peptide identifications were grouped into proteins by MASCOT, with no evidence of ambiguous protein assignment due to protein homology. The identified proteins were assigned to sub-cellular groups based on annotation in the SwissProt database, or using Mitoprot (score between 0.8 and 1.0) (22) and PSORT II Prediction (23) software.

NanoLC-QqTOF mass spectrometry and relative quantitation of peptides

The dried peptides recovered from solution IEF were separated on an LC packing HPLC system. The mixture was first desalted through a C18 300μm ID × 5 mm precolumn for 10 minutes and then introduced to a C18 PepMap 75 μm ID × 15 cm separation column. Peptide elution was accomplished with the same gradient described above. The effluent at a flow rate of 200nl/min was introduced into the Pulsar Plus ESI-qQTOF mass spectrometer (Applied BioSystems, Foster City, CA) via an uncoated 10μm ID SilicaTip needle held at 2400V. The mass spectrometer automatically scanned the m/z range 300–1500 Da at 1 second/scan. Data-dependent control was used to automatically perform MS/MS on the three most intense doubly or triply charged peptides detected in each MS scan. Previously selected precursor ions were excluded for 30 seconds. BioAnalyst software submitted the resulting MS/MS spectra to the SwissProt human database through a MASCOT in-house search engine (Matrix Science, London, UK) to identify peptides and thus their original proteins as above.

Relative Quantitation of Proteins

The abundance ratios of peptides in drug susceptible and the mitoxantrone resistant MCF-7 cells were determined based on peak area ratios in MS scans of labeled and unlabeled peptide pairs with at least one precursor identified by Mascot at the 95% confidence level. The calculation method was from Yao et. al, (27). The abundance ratios of each protein in Table 1 were estimated by averaging the (logarithms of the) relative abundance ratios of its constituent identified peptides in forward (and reverse) labeling analytical sample replicates. Proteins which exhibited at least a two fold abundance change were retained for statistical analysis.

Statistical analysis of protein abundance ratios

Confidence intervals for the relative protein abundance ratios of Table 1 were estimated by fitting a normal distribution to the $\log_2$ transformed peptide relative abundance ratios from each protein. Despite the small sample sizes, normal probability plots show reasonable agreement with the presumption of normality for most of the proteins (data not shown). Table 1 provides 95% confidence intervals about the relative protein abundance ratios for each of the forward and reverse analytical samples.

NIH-PA Author Manuscript

NIH-PA Author Manuscript

NIH-PA Author Manuscript

A two-sample T-test for samples with unequal variances was used to test the null hypothesis that the difference between the forward and reverse relative protein abundance ratios is due to experimental variation only. The T-test *p*-value (Table 1) quantifies the likelihood that the observed differences between the forward and reverse measurements could have been observed by chance events consistent with the observed experimental variation in the peptide relative abundance ratios.

RESULTS AND DISCUSSION

Peptide fractionation with solution isoelectric focusing

In this study, we applied sIEF using a device made of six chambers divided by five membranes with pH values of 3.0, 5.0, 6.5, 8.0 and 11 to fractionate peptide mixtures for the first dimensional separation, followed by reverse phase HPLC interfaced with a tandem mass spectrometer. The distinct profiles in the chromatograms of different fractions (not shown) indicate that the different cells contain different peptide mixtures. Among 637 peptides identified (see below), 80% were found in only one chamber, 15% were found in 2 fractions and 5% in 3 or 4 chambers. Reproducibility of sIEF fractionation was confirmed as satisfactory by overlaying three UV HPLC chromatograms of single fractions from three processed harvests. (18,28).

Peptide and protein identification using tandem mass spectrometry

The MS/MS spectra from the LC-LCQ instrument were submitted to the SwissProt human database through an in-house MASCOT search engine. Values of pI for all identified peptides were determined by the pI tool in Swiss-Prot database (www.expasy.org). The relationship between the calculated pI values and the pH values of the chambers in which peptides were found is presented in Figure 1.

Although the correlation is not perfect, the trend is correct, with peptides having more basic theoretical pI values concentrated in chambers with more basic pH ranges. It can be seen that good separation is achieved.

Assembling the unique peptides results in a total of 278 distinct proteins identified from 637 peptides in the mitochondrial soluble fraction. (See Supplementary Table 1.) Of the 278 proteins identified, 166, or 60%, have previously been categorized as mitochondrial proteins. There are also many mitochondrial-associated proteins, which are not annotated as mitochondrial proteins by SwissProt or other prediction software. For example, cathepsin D, which was known to be required for Bax insertion into the mitochondrial outer membrane during the apoptosis process (29), is classified as a lysosomal protein. The list of proteins identified in this study may offer evidence for other researchers when they study compartmental locations of proteins.

The distribution of calculated pI values and molecular weights of proteins identified in this study and annotated by SwissProt as mitochondrial, are illustrated in Figure 2. More than half of these proteins have pI values greater than 7, which is in agreement with the observations of other laboratories (30,31), who have suggested that cationic properties are needed for import into mitochondrial locations (e.g. inner membrane or matrix). It was also found that proteins with relatively low molecular weights (< 60kDa) dominate the set of identified proteins, which probably presents a characteristic of the soluble mitochondrial protein fraction.

The proteins identified here can also be compared with previous work in this laboratory, in which 2-D gel electrophoresis was used to analyze the soluble mitochondrial fraction from MCF-7 cells (32). About 100 more proteins were detected by the present method. Among proteins annotated as mitochondrial, 84 were identified in common by the two techniques, 48

NIH-PA Author Manuscript

NIH-PA Author Manuscript

NIH-PA Author Manuscript

were identified only in the gel workflow (32), and 82 were identified only in the shotgun strategy. Thus the two strategies are both overlapping and complementary in analyzing this complex protein mixture. It is estimated that half as much time was required for fractionation of an equivalent amount of sample by this two dimensional solution strategy, compared to the 2D-gel method used earlier in this laboratory.

Integration of ^{18}O labeling with solution isoelectric focusing (sIEF)

^{18}O labeling was integrated with solution isoelectric focusing and capillary LC-tandem mass spectrometry to study changes in mitochondrial proteins associated with drug resistance in MCF-7 human cancer cells. The proteins were extracted from mitochondrial pellets from MCF-7 drug susceptible and drug resistant cells. Each protein pool was determined to contain at least 1 mg total protein before it was digested into peptides. Aliquots corresponding to equivalent amounts of protein were drawn from each peptide pool and labeled: in the forward labeling protocol, the drug resistant sample with ^{16}O and the drug susceptible sample with ^{18}O; in the reverse labeling protocol, the drug resistant sample with ^{18}O and the drug susceptible sample with ^{16}O (27). The differentially labeled samples were pooled and fractionated by solution IEF. Each pI fraction was then injected for analysis of the isotope ratios by nanoHPLC-ESI-qQTOF. Some examples of these spectra are shown in Figures 3 and 4, and discussed further below. Ratios of $^{16}O/^{18}O$ lower than 0.5 or higher than 2.0 were considered for further investigation. The majority of the identified proteins did not show significantly altered abundances in mitoxantrone-resistant MCF-7 cells (See Supplementary Table 1).

Implementation of forward and reverse ^{18}O labeling

With the objective to improve accuracy in protein quantitation, a forward and reverse isotope labeling method was proposed and demonstrated with $^{18}O/^{16}O$ by Wang et al (33). More recently, this strategy was evaluated by Cantin et al (17), using ^{15}N metabolic labeling, who report that the forward and reverse experiments provided highly inconsistent measurements. Reverse labeling is evaluated again in the present project. The inverse labeling experiments were performed in parallel. Each peptide mixture was fractionated and analyzed by the same strategy, described above. As a result, an inverted labeling pattern is produced between the two parallel experiments, as is illustrated in Figure 3. The characteristic pattern of a 2 Da mass shift for doubly-charged ions can be seen in both spectra. The observed intensity ratios ($^{16}O/^{18}O$) are approximately reciprocal between two labeling strategies. It is difficult to obtain complete labeling for every peptide in the mixture, because, different peptides have different ^{18}O exchange rates (34). Back exchange may also contribute to variation, although enzyme-catalyzed back exchange is minimized in the procedure used here by filtering out the immobilized trypsin. Forward and reverse labeling makes it possible to check for any systematic bias introduced by the labeling direction. Such bias cannot be estimated using an equivalent number of forward only, or reverse only, experiments.

In addition, the reverse labeling experiment is especially useful for those situations where the change in abundance of a protein is so large that it is detected in one sample but not in the other. Figure 4 demonstrates this benefit. The two peptides ELSEALGQIFDSQR and SDLAVPSELALLK both originate from galectin-3 binding protein. In the forward labeling experiments, the ions at m/z 796.9 and 678.4 appear not to be part of isotope pairs, and might be assigned as contaminants. However, they are clearly detected in the reverse labeling experiment as peptides derived from a protein whose abundance is altered beyond the dynamic range of the mass spectrum. It should be noted that the dynamic range for this measurement is about 10:1.

NIH-PA Author Manuscript

NIH-PA Author Manuscript

NIH-PA Author Manuscript

It should also be noted that peptides carrying two ^{18}O labels produce CID spectra that contain y series ions with masses 4 Da heavier than normal. Such spectra do not usually provide identifications in database searches, unless a specific ^{18}O C-terminus variable modification setting is used. When the peptide is detectable in only one sample, only one labeling direction will be suitable for identification without the use of this specialized search engine parameter.

Mitochondrial protein abundance profile in the MCF-7 cell line resistant to mitoxantrone

Forward and reverse ^{18}O labeling experiments integrated with solution isoelectric focusing and LC-MS were used to compare the protein abundance profiles from the drug-susceptible MCF-7 cell line and the subline selected for resistance to mitoxantrone. Each peptide ratio could potentially be observed in a sIEF fraction in as many as 12 different analytical samples, as shown in Scheme 1, and in many cases, multiple peptides were observed from each protein. The peptide ratio observations from each of the forward and reverse analytical samples, for each protein, were averaged (after $\log_2$ transformation) and a 95% confidence interval was estimated. Table 1 lists proteins whose confidence intervals indicate at least a two-fold change.

A number of proteins show abundance ratios well above 2, including the Galectin-3 binding protein (Q08380), which is only detected in the mitoxantrone resistant cell-line. The repeated ratio observations make it possible to estimate not only the differential abundance ratios between mitoxantrone resistant and drug susceptible MCF-7 cell-lines, but also to provide confidence intervals for the differential abundance ratio estimates and to check for systematic biases introduced by the experimental protocol. For some of the proteins in Table 1, there is no evidence of any such systematic bias, while for others the difference in protein abundance ratios estimated by forward and reverse labeling is highly significant.

In this study, incomplete labeling, as previously discussed, would inflate the apparent relative abundance ratio of forward labeled analysis samples, and decrease the relative abundance ratio of reverse labeled samples. In Table 1, we observe that, with one exception (P54886), all of the proteins with statistically significant ($p<0.05$) differences between forward and reverse labeling ratios have the forward ratio larger than the reverse ratio.

The strength of this analysis is not the absence of these effects, but use of structured repeat observations so that these biases can be explicitly observed.

Biological implications of changes in protein abundances

Of particular interest are the several proteins shown to have altered abundances in the mitoxantrone resistant (MX) cell line as shown in Table 1.

We observed significant increases in the abundances of apoptosis inhibitor 5 (API-5) and prohibitin in MX cells. Both are reported to be potent suppressors of the E2F-dependent apoptotic pathway (45,46), and our observations are consistent with decreased susceptibility to the chemotherapeutic agent.

Galectin-3 binding protein was originally described as a tumor-secreted antigen in human breast cancer cells (35) and then reported to participate in the immune defense against cancer (36). Galectin-3 itself is reported to regulate tumor proliferation, angiogenesis and apoptosis and has shown anti-apoptotic function in certain cell types (37–39). Yu et al. have demonstrated that galectin-3 is translocated to perinuclear mitochondrial membranes from the cytoplasm and inhibits cytochrome C release following a variety of apoptotic stimuli (40). It has already been suggested that galectin-3 may confer resistance to chemotherapy (40–44). In our research galectin-3 binding protein was found in the mitoxantrone resistant (MX) cell line at an abundance >10 times that in the drug susceptible cell line. This suggests that galectin-3 binding protein is upregulated or redistributed in MX cells, and contributes to evasion of apoptosis and

NIH-PA Author Manuscript

NIH-PA Author Manuscript

NIH-PA Author Manuscript

cell survival. The mechanism and consequences of the increased abundance of galectin-3 binding protein in the mitochondria of mitoxantrone resistant MCF-7 cells are the subject of on-going research.

CONCLUSIONS

We have integrated forward and reverse ^{18}O-labeling with a two dimensional separation strategy, throughout which the sample remains in solution. This combination appears well-suited for sensitive and automated quantitative comparisons. Reversed ^{18}O-labeling experiments were carried out to improve the precision and dynamic range of the method. The biological and analytical sample replicates made it possible to check for a systematic bias due to the experimental protocol and to provide protein abundance ratio estimates with 95% confidence intervals. The overall strategy identified twelve mitochondrial proteins with abundances altered significantly in drug resistant cells. Most interesting among these is galectin-3 binding protein, here associated for the first time with acquired drug resistance.

Supplementary Material

Refer to Web version on PubMed Central for supplementary material.

Acknowledgements

This work was supported by the National Institutes of Health (GM 21248 and CA 126189). We thank Drs. K. H. Cowan (Eppley Cancer Center, University of Nebraska) for cell lines, Dr. R. Strong for helpful discussions, and Mr. A. Chertov for technical assistance. Part of this work was performed at the University of Maryland Greenebaum Cancer Center Proteomics Core Facility.

References

1. Zang L, Toy DP, Hancock WS, Sgroi DC, Karger BL. J Proteome Research 2004;3:604–612. [PubMed: 15253443]
2. Gronborg M, Bunkenborg J, Kristiansen TZ, Jensen ON, Yeo CJ, Hruban RH, Maitra A, Goggins MG, Pandey A. J Proteome Research 2004;3:1042–1055. [PubMed: 15473694]
3. Hood BL, Lucas DA, Kim G, Chan KC, Blonder J, Issaw HJ, Veenstra TD, Conrads TP, Pollet I, Karsan A. J Amer Soc Mass Spectrom 2005;16:1221–1230. [PubMed: 15979327]
4. Wolters DA, Washburn MP, Yates JR. Anal Chem 2001;73:5683–5690. [PubMed: 11774908]
5. Link AJ, Eng J, Schieltz DM, Carmack E, Mize GJ, Morris DR, Barvik BM, Yates JR. Nature Biotech 1999;17:676–682.
6. Xiong L, Andrews P, Regnier FE. J Proteome Res 2003;2:618–625. [PubMed: 14692455]
7. Geng M, Ji J, Regnier F. J Chromatogr A 2000;870:295–313. [PubMed: 10722087]
8. Jensen PK, Pasa-Tolic L, Anderson GA, Horner JA, Lipton MS, Bruce JE, Smith RD. Anal Chem 1999;71:2076–2084. [PubMed: 10366890]
9. Zhang CX, Xiang F, Pasa-Tolic L, Anderson GA, Veenstra TD, Smith RD. Anal Chem 2000;72:1462–1468. [PubMed: 10763241]
10. Wall DB, Kachman MT, Gong S, Hinderer R. Anal Chem 2000;72:1099–1111. [PubMed: 10740846]
11. Cargile BJ, Sevinsky JR, Essader AE, Stephenson JL, Bundy JL. J Biomol Tech 2005;16:181–189. [PubMed: 16461941]
12. Moritiz RL, Schutz F, Connolly LM, Kapp EA, Speed TP, Simpson RJ. Anal Chem 2004;76:4811–4824. [PubMed: 15307793]
13. Xie H, Bandhakavi S, Griffin TJ. Anal Chem 2005;77:3198–3207. [PubMed: 15889909]
14. Zuo X, Speicher DW. Anal Biochem 2000;284:266–278. [PubMed: 10964409]
15. Righetti PG, Wenisch E, Faupel M. J Chromatogr 1989;475:293–309.
16. Zhu Y, Lubman DM. Electrophoresis 2004;25:949–58. [PubMed: 15095432]

NIH-PA Author Manuscript

NIH-PA Author Manuscript

NIH-PA Author Manuscript

17. Cantin GT, Venable JD, Coclorva D, Yates JR. J Proteome Res 2006;5:127–134. [PubMed: 16396503]
18. An Y, Fu Z, Gutierrez P, Fenselau C. J Proteome Res 2005;4:216–232.
19. Solary E, Bettaieb A, Dubrez-Daloz L, Corcos L. Leuk Lymphoma 2003;44:563–574. [PubMed: 12769332]
20. Vo TD, Palsson BO. Am J Physiol Cell Physiol 2007;292:C164–C177. [PubMed: 16885397]
21. Rigobello MP, Donella-Deana A, Cesaro L, Bindoli A. Biochem J 2001;356:567–570. [PubMed: 11368786]
22. http://ihg.gsf.de/ihg/mitoprot.html.
23. http://psort.nibb.ac.jp/cgi-bin/runsport.pl.
24. Reifschneider NH, Goto S, Nakamoto H, Takahashi R, Sugawa M, Dencher NA, Krause F. J Proteome Res 2006;5:1117–1132. [PubMed: 16674101]
25. Johnson DT, Harris RZ, Blair PV, Balaban RS. Am J Physiol Cell Physiol 2007;292:C698–C707. [PubMed: 16971502]
26. McDonald TG, Van Eyk JE. Basic Res Cardiol 2003;98:219–227. [PubMed: 12835951]
27. Yao X, Freas A, Ramirez J, Demirev PA, Fenselau C. Anal Chem 2001;73:2836–2842. [PubMed: 11467524]correction in Anal. Chem. 2004, 76, 2675
28. Wang, J. PhD Thesis. University of Maryland; 2007. Integration of ^{18}O Labeling and Solution Isoelectric Focusing in a Shotgun Analysis of Mitochondrial Proteins.
29. Jaattela M, Cande C, Kroemer G. Cell Death Differ 2004;11:135–136. [PubMed: 14647234]
30. Taylor SW, Fahy E, Zhang B, Glenn GM, Warnock DE, Wiley S, Murphy AN, Gaucher SP, Capaldi RA, Gibson BW, Ghosh SS. Nature Biotech 2003;21:281–286.
31. Abad MF, DiBenedetto G, Magalhaes PJ, Filippin L, Pozzan T. J Biol Chem 2004;279:11521–11529. [PubMed: 14701849]
32. Strong R, Nakanishi T, Ross D, Fenselau C. J Proteome Res 2006;5:2389–2395. [PubMed: 16944951]
33. Wang YK, Ma Z, Quinn DF, Fu EW. Anal Chem 2001;73:3742–3750. [PubMed: 11510843]
34. Yao X, Afonso C, Fenselau C. J Proteome Res 2003;2:147–152. [PubMed: 12716128]
35. Iacobelli S, Arno S, D'Orazio A, Coletti G. Cancer Res 1986;46:3005–3010. [PubMed: 3516389]
36. Ullrich A, Sures I, D'Egidio M, Jallal B, Powell TJ, Herbst R, Dreps A, Azam M, Rubinstein M, Natoli C, Shawver LK, Schlessinger J, Iacobelli S. J Biol Chem 1994;269:18401–18407. [PubMed: 8034587]
37. Yang R, Hsu DK, Liu F. Proc Natl Acad Sci USA 1996;93:6737–6742. [PubMed: 8692888]
38. Akahani S, Nangia-Makker O, Inohara H, Kim H, Raz A. Cancer Res 1997;57:5272–5276. [PubMed: 9393748]
39. Jung EJ, Moon HG, Cho BI, Jeong CY, Joo YT, Lee YJ, Hong SC, Choi SK, Ha WS, Kim JW, Lee CW, Lee JS, Park ST. Int J Cancer 2007;120:2331–2338. [PubMed: 17304502]
40. Yu F, Finley RL, Raz A, Kim HC. J Biol Chem 2002;277:15819–15827. [PubMed: 11839755]
41. Takenaka Y, Fukumori T, Yoshii T, Oka N, Inohara H, Kim HC, Bresalier RS, Raz A. Mol Cell Biol 2004;24:4395–4406. [PubMed: 15121858]
42. Fukumori T, Oka N, Takenaka Y, Nangia-Makker P, Elsamman E, Kasai T, Shono M, Kanayama H, Ellerhorst J, Lotan R, Raz A. Cancer Res 2006;66:3114–3119. [PubMed: 16540661]
43. Prieto VG, Mourad-Zeidan AA, Melnikova V, Johnson MM, Lopez A, Diwan H, Lazar AJF, Shen SS, Zhang PS, Reed JA, Gershenwald JE, Raz A, Bar-Eli M. Clin Cancer Res 2006;12:6709–6715. [PubMed: 17121890]
44. Dowling P, Meleady P, Dowd A, Henry M, Glynn S, Clynes M. Biochimica et Biophyica Acta 2006;1774:93–101.
45. Morris E, Michaud WA, Ji J, Moon N, Rocco JW, Dyson NJ. PloS Genetics 2006;2:1836–1848.
46. Fusaro G, Dasgupta P, Rastogi S, Joshi B, Chellappan S. J Biol Chem 2003;278:47853–47861. [PubMed: 14500729]

NIH-PA Author Manuscript

NIH-PA Author Manuscript

NIH-PA Author Manuscript

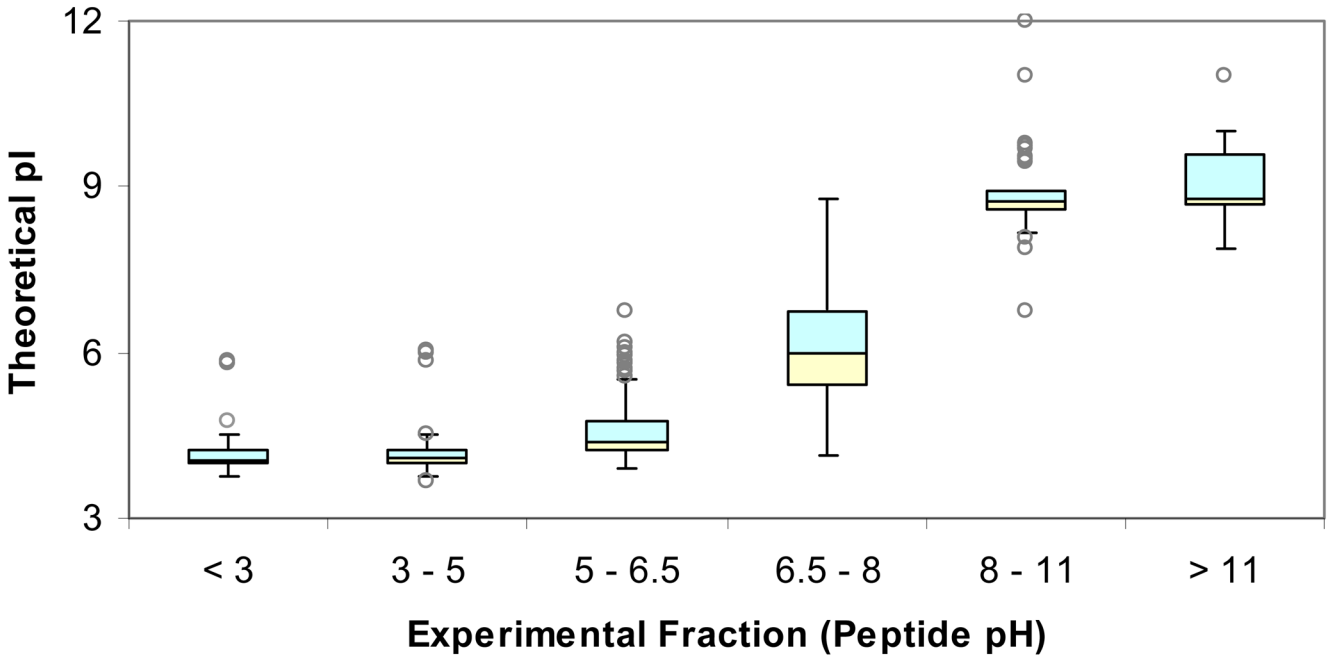

Figure 1.
The relationship between peptide pI and chamber pH defined by Immobiline boundary membranes is presented. Each box-plot shows the distribution of theoretical pI values of identified peptides in a particular experimental fraction. The bottom, top, and internal division of the box indicates the 1st and 3rd quartiles, and the median of the data, respectively. The lower (upper) whisker indicates the minimum (maximum) non-outlier observation. Outliers are indicated with dots

NIH-PA Author Manuscript

NIH-PA Author Manuscript

NIH-PA Author Manuscript

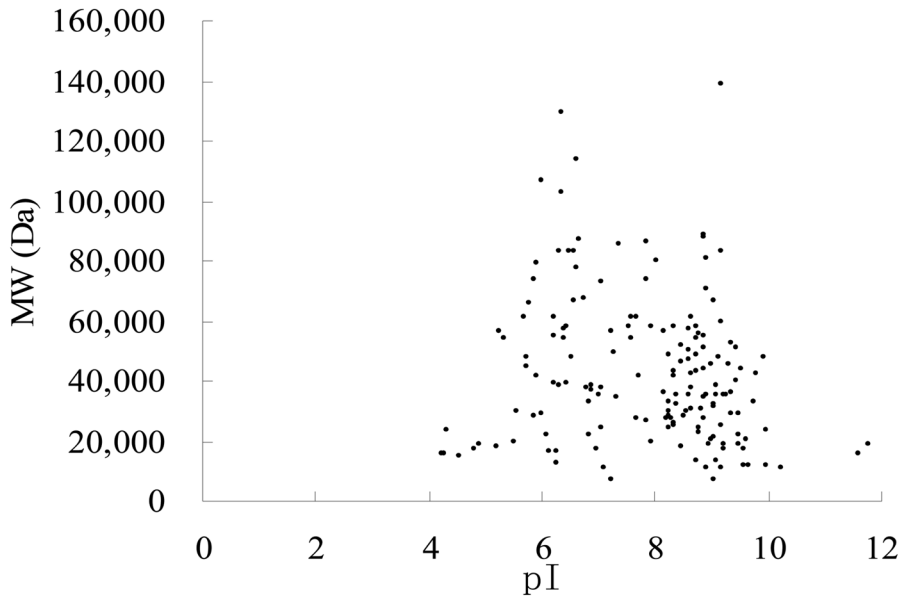

Figure 2.
Identified Proteins annotated as mitochondrial in SwissProt, plotted according to pI and molecular weight.

NIH-PA Author Manuscript

NIH-PA Author Manuscript

NIH-PA Author Manuscript

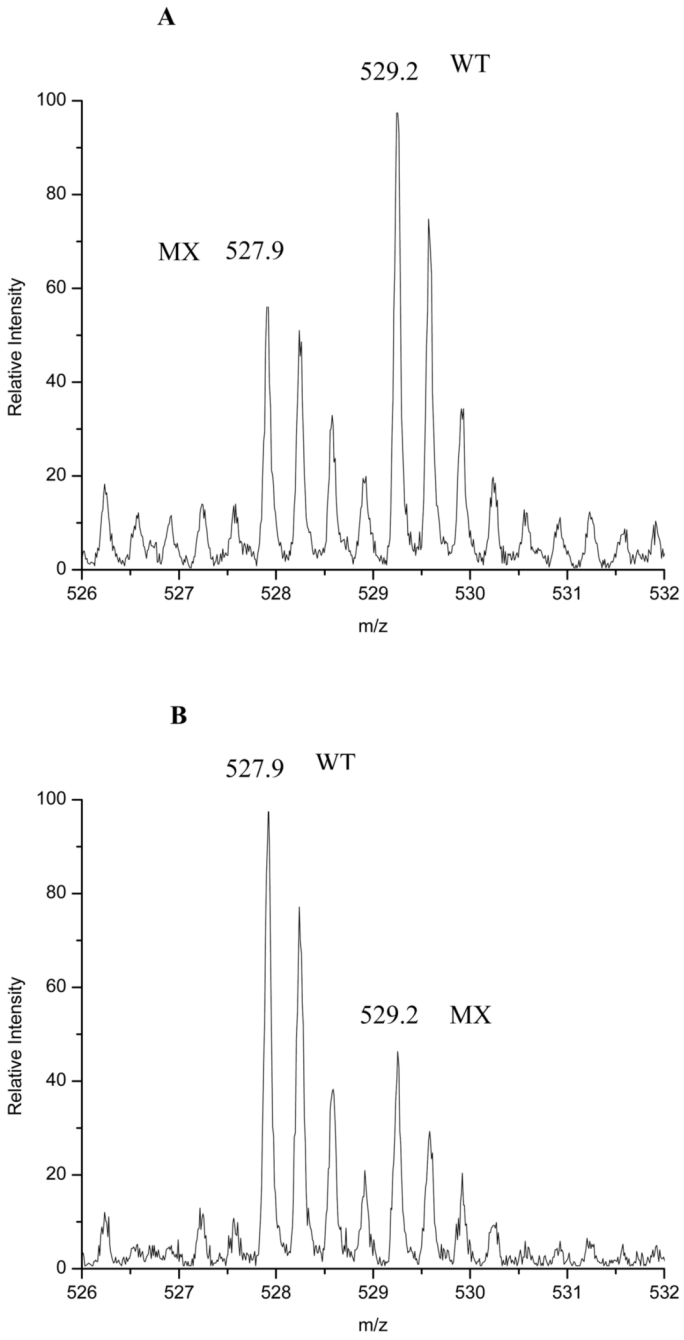

Figure 3.
Partial mass spectra of the same peptide pair from inverse labeling experiments. This doubly-charged peptide was identified as SEEQLKEEGIEYK, originating from mitochondrial protein dihydrolipoyl dehydrogenase. A: Forward labeling experiment; B: Reverse labeling.

NIH-PA Author Manuscript
NIH-PA Author Manuscript
NIH-PA Author Manuscript

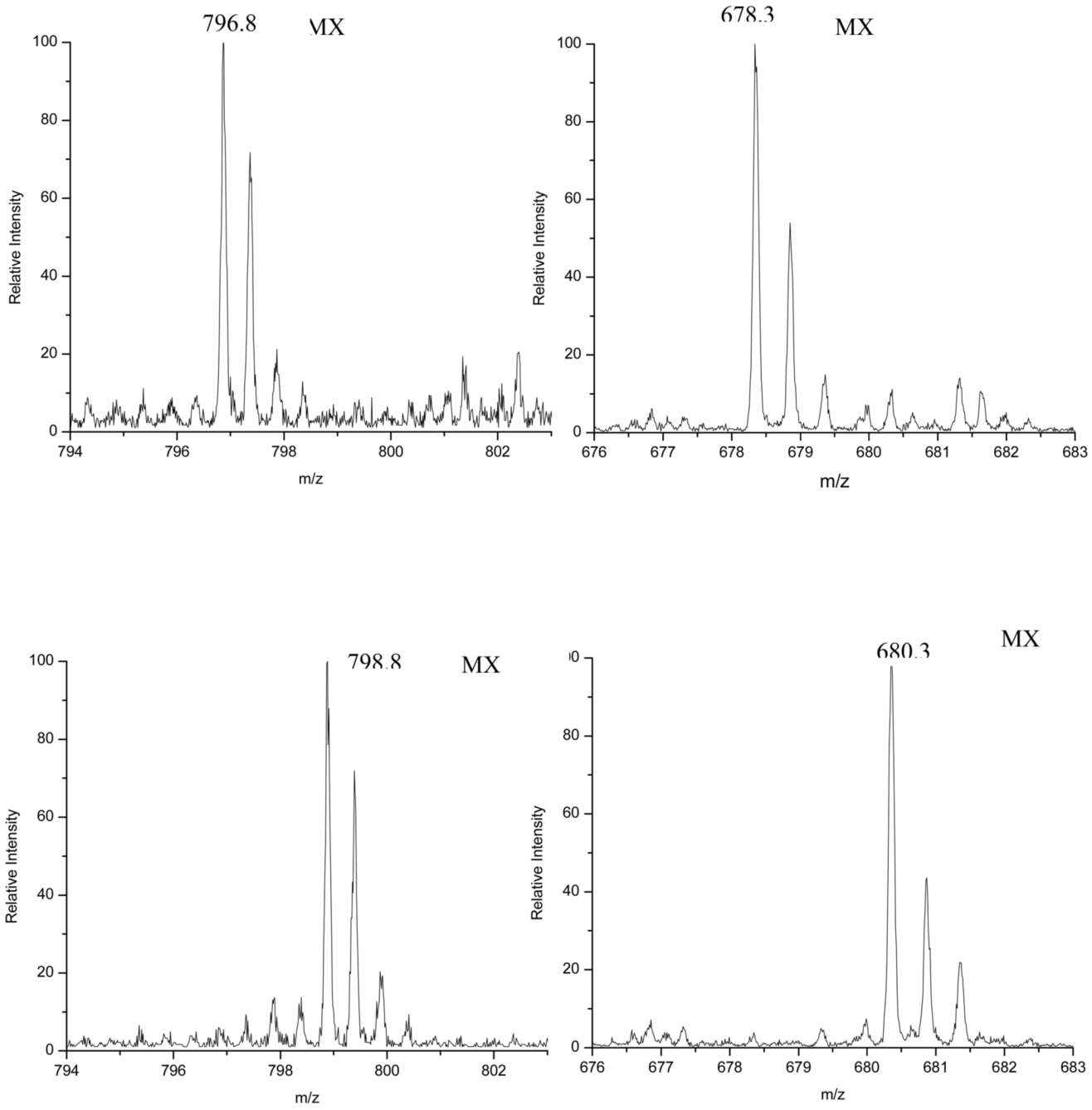

Figure 4.

Partial mass spectra of peptide pairs from inverse labeling experiments. Both peptides are derived from galectin-3 binding protein.

Upper left panel: peptide ELSEALGQIFDSQR forward labeling experiment;
Lower left panel: peptide ELSEALGQIFDSQR reverse labeling experiment;
Upper right panel: peptide SDLAVPSELALLK forward labeling experiment;
Lower right panel: peptide SDLAVPSELALLK reverse labeling experiment.

NIH-PA Author Manuscript

NIH-PA Author Manuscript

NIH-PA Author Manuscript

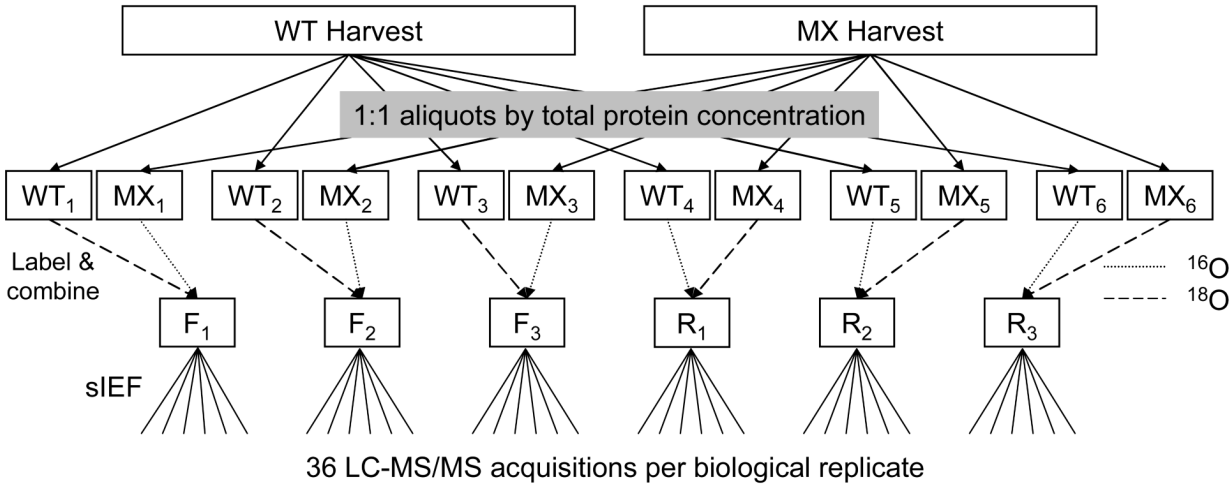

Scheme 1.

Analytical sample replicate structure. Wild-type (WT) and mitoxantrone resistant MCF-7 cell-line harvests (MX); analytical replicates of forward (F_1, …, F_3) and reverse (R_1, …, R_3) ^{18}O labeling shown. Solution isoelectric focusing (sIEF) applied to all analytical replicates (F_1, …, F_3, R_1, …, R_3), resulting in 36 LC-MS/MS acquisitions per biological replicate.

NIH-PA Author Manuscript NIH-PA Author Manuscript NIH-PA Author Manuscript

Table 1

Proteins with altered abundances between the mitoxantrone resistant (MX) and drug susceptible (WT) MCF-7 cell lines.

Accession	Protein name	Peptides/Observations	Forward Ratio (WT/MX) [a]	Reverse Ratio (WT/MX) [a]	T-test *p*-value [b]
Q9HCCO	Methylcrotonoyl-CoA carboxylase beta chain	2/15	2.37 [2.00,2.80]	1.90 [1.74,2.06]	0.018
P49411	Elongation factor Tu	5/29	2.46 [2.07,2.93]	2.12 [1.79,2.53]	0.20
P20674	Cytochrome C oxidase polypeptide Va	2/6	3.84 [2.24,6.58]	1.88 [1.52,2.32]	0.019
P54886	Delta 1-pyrroline-5-carboxylate synthetase	1/11	2.15 [2.06,2.24]	2.88 [2.59,3.20]	0.00059
Q16698	2, 4-dienoyl-CoA reductase	1/10	3.37 [3.12,3.63]	2.18 [2.11,2.26]	1.1e-05
P35232	Prohibitin	6/15	2.70 [2.44,2.98]	2.44 [2.35,2.54]	0.055
Q9BZZ5	Apoptosis inhibitor 5	1/10	3.07 [2.57,3.67]	2.34 [2.05,2.67]	0.011
Q92665	Mitochondrial 28S ribosomal protein S31	1/10	3.16 [2.51,3.97]	2.16 [1.78,2.61]	0.008
P82650	Mitochondrial 28S ribosomal protein S22	1/9	2.86 [2.63,3.11]	2.51 [1.80,3.50]	0.31
Q08380	Galectin-3 binding protein	2/17	Only detected in MX	Only detected in MX	
P09622	Dihydrolipoyl dehydrogenase	3/21	0.50 [0.45,0.55]	0.41 [0.36,0.47]	0.022
Q9HAV7	GrpE protein homolog 1	2/11	0.54 [0.44,0.66]	0.39 [0.36,0.43]	0.0086

[a] with 95% confidence interval;

[b] *p*-value of two-sample T-test for different forward and reverse ratio.